The Thirty-Seventh AAAI Conference on Artificial Intelligence (AAAI-23)

FoPro: Few-Shot Guided Robust Webly-Supervised Prototypical Learning

Yulei Qin[*1], **Xingyu Chen**[*1], **Chao Chen**[1], **Yunhang Shen**[1], **Bo Ren**[1],
Yun Gu[2], **Jie Yang**[2], **Chunhua Shen**[3]

[1]Tencent YouTu Lab
[2]Shanghai Jiao Tong University
[3]Zhejiang University
{yuleiqin, harleychen, aaronccchen, odysseyshen, timren}@tencent.com,
yungu@ieee.org, jieyang@sjtu.edu.cn, chunhuashen@zju.edu.cn

Abstract

Recently, webly supervised learning (WSL) has been studied to leverage numerous and accessible data from the Internet. Most existing methods focus on learning noise-robust models from web images while neglecting the performance drop caused by the differences between web domain and real-world domain. However, only by tackling the performance gap above can we fully exploit the practical value of web datasets. To this end, we propose a Few-shot guided Prototypical (FoPro) representation learning method, which only needs a few labeled examples from reality and can significantly improve the performance in the real-world domain. Specifically, we initialize each class center with few-shot real-world data as the "realistic" prototype. Then, the intra-class distance between web instances and "realistic" prototypes is narrowed by contrastive learning. Finally, we measure image-prototype distance with a learnable metric. Prototypes are polished by adjacent high-quality web images and involved in removing distant out-of-distribution samples. In experiments, FoPro is trained on web datasets with a few real-world examples guided and evaluated on real-world datasets. Our method achieves the state-of-the-art performance on three fine-grained datasets and two large-scale datasets. Compared with existing WSL methods under the same few-shot settings, FoPro still excels in real-world generalization. Code is available at https://github.com/yuleiqin/fopro.

Introduction

The past decade has witnessed a revolution in computer vision with the advent of large-scale labeled datasets (*e.g.*, ImageNet (Deng et al. 2009)). However, a large collection of data are sometimes inaccessible, let alone the time-consuming and expensive annotations. On the contrary, there are abundant weakly labeled images on the Internet. Therefore, webly supervised learning (WSL) has attracted growing attention from researchers (Krause et al. 2016; Kaur, Sikka, and Divakaran 2017; Kolesnikov et al. 2019; Zhang et al. 2020; Tu et al. 2020; Liu et al. 2021; Zhang et al. 2021).

Queries and tags are directly used as weak labels without verification, bringing about a considerable proportion of noises in web datasets (*e.g.*, 20% in JMT-300M (Sun et al. 2017), 34% in WebVision (Li et al. 2017), and 32% in WebFG496 (Sun et al. 2021)). As shown in Fig. 1(a), various noises include label flipping errors, semantic ambiguity of polysemy queries, and outliers of unknown categories. To alleviate their effect, prior knowledge such as neighbor density (Guo et al. 2018), reference clean sets (Jiang et al. 2018; Lee et al. 2018), and side information (Zhou et al. 2020; Cheng et al. 2020) is explored for label correction and sample selection. Recently, Li *et al.* (Li, Xiong, and Hoi 2020) develop a self-supervised method with representative class prototypes (MoPro) to achieve satisfying performance.

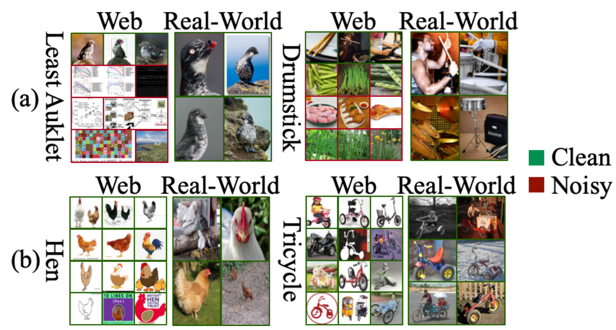

Figure 1: Differences between web and real-world images. (a) Web dataset noise. (b) Web dataset bias.

Most existing WSL methods are merely concerned with noise reduction. They ignore the model degradation in real-world scenarios because the performance on web domain testing sets is emphasized in previous model assessments. Domain gaps exist between images crawled from the web (*e.g.*, advertising photos, artworks, and rendering) and those captured in reality (see Fig. 1(b)). In this case, the better fitting of web images counteractively leads to worse generalization on practical applications. Few studies try to tackle such performance gaps by domain adaptation methods. For example, Xu *et al.* (Xu et al. 2016) distill knowledge from the web domain to the real-world domain. Niu *et al.* (Niu, Li, and Xu 2015) fine-tune pretrained models on real-world datasets. However, both of them need plenty of labeled data in the target domain, which impedes practicability.

Unlike the methods above, our objective is to cost-efficiently mine web data for real-world applications. We

[*]These authors contributed equally.

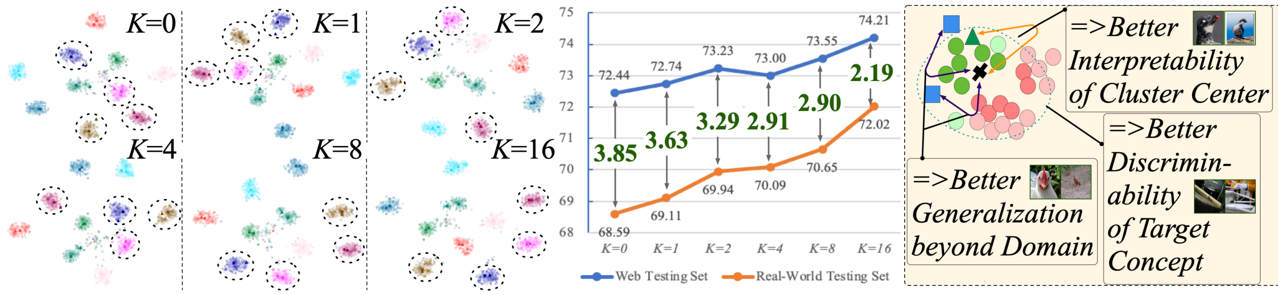

(a) Effect of Few-Shots for Guidance (b) Performance Gap (c) Mechanism of FoPro

Figure 2: (a) The t-SNE (Van der Maaten and Hinton 2008) of the low-dimensional embeddings of web images (○) substantiates that with the increase of K, class prototypes ($\times$) are regularized to approach few shots (Δ) with dense intra-class and isolated inter-class distribution. (b) The diminished performance gap between the testing results of web (WebVision1k) and real-world (ImageNet1k) images confirms that FoPro takes full advantage of few shots to improve its generalization beyond the web domain, making web data truly useful in learning representations for actuality. (c) FoPro estimates noise-robust prototypes to pull instances nearby closer. Noisy samples are filtered by assessing their relation with prototypes. Only clean ones update prototypes in return. FoPro achieves better interpretability, discriminability, and generalization. Best viewed magnified.

handle both the noise and domain gap by resorting to a few human-labeled samples for guidance on *whom to learn from* and *what to learn*. In our setting, clean labeled examples are too scarce to train or fine-tune a deep model, and therefore alternative methods need to be developed in response.

To this end, we propose a robust prototypical representation learning method with noisy web data and a few clean examples (see Fig.2). Motivated by the anchoring role of class prototypes (Li et al. 2020; Li, Xiong, and Hoi 2020), we introduce **F**ew-sh**o**t guided **Pro**totypes, termed as **FoPro**, to effectively deal with noise and domain gap. Technically, we project features of the penultimate layer of a classification model to low-dimensional embeddings. The critical problem is how to *formulate a class-representative and domain-generalized prototype* in the embedding space without being deviated by the dominating noises. Due to noise memorization (Arpit et al. 2017), simply averaging over instances with high prediction confidence does not promise a noise-robust estimation. Consequently, we first initialize each class prototype with realistic few shots as the cluster center. Secondly, intra-class distance is shortened by contrastive learning between web instances and prototypes. Then, high-quality web examples are involved in polishing prototypes to improve discriminability. Simultaneously, high similarity between prototypes and few shots is regularized to maximize the interpretability and generalizability of prototypes. Finally, we quantify the compatibility between instances and prototypes by the proposed relation module for sample selection and correction, which benefits prototype update in the next iteration. Specifically, the relation module learns a flexible and transferable metric to assess if a web image corresponds to its label. Besides, we set siamese encoders (He et al. 2020) and prototypes are only updated by the momentum encoder in a smooth and progressive way.

Our contributions can be summarized as follows:

- We propose a new few-shot learning setting in WSL with abundant noisy web images and a few real-world images, which aims to improve the performance of WSL for real-world applications in a cost-efficient way.
- We present a new method under the setting above called FoPro, which simultaneously solves noise and data bias in an end-to-end manner. Experimental results show that our method can significantly improve the performance in real-world benchmark datasets.
- We propose a new relation module for label noise correction. It outperforms existing methods that use fixed metrics (*e.g.*, cosine distance) by evaluating instance-prototype similarity with a learnable metric.
- Extensive experiments on the fine-grained WebFG496 and the large-scale WebVision1k datasets confirm the superiority of FoPro over the state-of-the-art (SOTA) methods. Performance under the increasing K-shot settings demonstrates that FoPro utilizes few shots wisely to bridge the gap towards real-world applications.

Related Work

Webly Supervised Learning

WSL aims to leverage vast but weakly-annotated web resources. Previous works utilize web images for tasks including classification (Bergamo and Torresani 2010; Wu et al. 2021; Yao et al. 2017, 2020), detection (Divvala, Farhadi, and Guestrin 2014; Shen et al. 2020), and segmentation (Shen et al. 2018; Jin, Ortiz Segovia, and Susstrunk 2017).

Recently, noise cleaning methods such as self-contained confidence (SCC) (Yang et al. 2020) and momentum prototype (MoPro) (Li, Xiong, and Hoi 2020) are proposed to improve representation learning in WSL. SCC balances two supervision sources from web labels and predicted labels by introducing instance-wise confidence. MoPro targets model pretraining for several down-streaming tasks by combining self-supervised and webly-supervised techniques. Specifically, MoPro is closely related to ours since the contrast between instances and prototypes is used to learn discriminative features. Different from MoPro, we formulate a brand-new setting where a few samples labeled by experts are available. To assure that class prototypes are not misled by noise, an implicit constraint on distribution is achieved by enforcing high similarity between prototypes and few shots. Furthermore, we estimate the relation score between instances and prototypes to correct labels and discard out-of-distribution (OOD) samples.

Learning from Noisy Labels

Labels in human-annotated datasets can still be noisy due to lack of expert domain knowledge (Song et al. 2022). To prevent deep models from overfitting noisy labels, several studies have been conducted and can be categorized as: 1) robust architecture (*e.g.*, noise transition layer (Chen and Gupta 2015) and probability model (Xiao et al. 2015)); 2) regularization techniques (*e.g.*, label smoothing (Pereyra et al. 2017) and mix-up (Zhang et al. 2018)); 3) robust losses (*e.g.*, MAE (Ghosh, Kumar, and Sastry 2017) and GCE (Zhang and Sabuncu 2018)); 4) loss refinement (*e.g.*, reweighting (Wang, Liu, and Tao 2017) and bootstrapping (Reed et al. 2015)); 5) sample selection (*e.g.*, multi-model collaboration (Malach and Shalev-Shwartz 2017) and iterative strategies (Li, Socher, and Hoi 2019)). Hybrid approaches are designed in practice. For example, PeerLearn (Sun et al. 2021) develops a two-stage framework with peer models. Each model chooses clean samples independently and feeds them to train the other model. Different from the existing methods, we do not assume that samples with small losses or high confidence are clean. Instead, we maintain class prototypes and filter out noise by comparing instances and prototypes in a non-linear metric. Moreover, PeerLearn presumes that the percentage of noise is consistent across categories, which contradicts our observation.

Contrastive Representation Learning

Contrastive learning methods can be roughly categorized as: 1) context-instance contrast, where the relationship of local parts with respect to global context is learned (Kim et al. 2018); 2) instance-wise contrast, where similar image pairs are pulled closer with dissimilar pairs pushed farther (He et al. 2020; Chen et al. 2020a). Prototypical contrastive learning (PCL) (Li et al. 2020) encourages each image embedding to be adjacent to its assigned cluster prototype. However, their method is under an unsupervised setting where k-means clustering is used to generate prototypes. Our model is supervised by both numerous-yet-noisy web labels and limited-yet-clean few-shot labels. Besides, in PCL, batch embeddings in the current epoch are contrasted with the "outdated" prototypes in the previous epoch. FoPro keeps modifying prototypes smoothly all the time so that clean samples can be pinpointed by the latest features.

Method

In this section, a formal description of our few-shot WSL setting is presented, followed by the detailed explanation of FoPro. Fig. 3 illustrates the model architecture.

Problem Statement

Existing WSL setting aims to train a deep model $\mathcal{F}(\theta_e;\theta_c)$ with the optimal parameters of encoder θ_e^* and classifier θ_c^* from the web dataset $D^w = \{(\mathbf{x}_i^w, y_i^w)\}_{i=1}^{N^w}$. Here, $\mathbf{x}_i^w$ denotes an image, $y_i^w \in \{1,...,C\}$ is its class label. The number of classes and images are C and N^w, respectively. Due to noise issues, y_i^w might not equal to the ground-truth y_i^*. If $y_i^w \neq y_i^*$ and $y_i^* \in \{1,...,C\}$, $(\mathbf{x}_i^w, y_i^w)$ is viewed as an in-distribution (IND) sample with label-flipping error. If $y_i^w \neq y_i^*$ and $y_i^* \notin \{1,...,C\}$, then $(\mathbf{x}_i^w, y_i^w)$ is an out-of-distribution (OOD) sample.

We propose a new WSL setting that additional real-world images are available with verified labels: $D^t = \{(\mathbf{x}_i^t, y_i^t)\}_{i=1}^{N^t}$ and $y_i^t = y_i^*$. The number of real-world samples is $N^t = K \cdot C$, where K denotes K-shot per class. Our FoPro aims to achieve two goals with D^w: 1) to learn generalizable representations from high-quality examples; 2) to correct IND samples and discard OOD samples.

Model Architecture

The main components of FoPro include siamese encoder backbones, a classifier, a projector, a reconstructor, an auxiliary classifier, and a relation module.

Our siamese encoder networks share the same architecture. Enlighted by MoCo (He et al. 2020), we update parameters of the first encoder θ_e^1 by back-propagation and employ momentum update for the second encoder θ_e^2:

$$\theta_e^2 = m_e\theta_e^2 + (1 - m_e)\theta_e^1, \tag{1}$$

where m_e is the momentum parameter. The plain and momentum encoders respectively extract features $\mathbf{v}_i^{\{w;t\}}$ and $\mathbf{v}_i'^{\{w;t\}} \in \mathbb{R}^{d_e}$ from inputs $\mathbf{x}_i^{\{w;t\}}$ and their augmented counterparts $\mathbf{x}_i'^{\{w;t\}}$. Note that our encoder is structure-agnostic, and its choices are up to specific tasks. All layers except the last fully connected (FC) layer are used.

A classifier is trained to map features $\mathbf{v}_i^{\{w;t\}}$ to the predicted probabilities $\mathbf{p}_i^{\{w;t\}}$ over C classes. It consists of one FC layer with softmax activation.

A projector distills discriminative contents from features $\mathbf{v}_i^{\{w;t\}}$ for low-dimensional embeddings $\mathbf{z}_i^{\{w;t\}} \in \mathbb{R}^{d_p}$. It is composed of two FC layers and one ReLU layer. We follow (Chen et al. 2020a,b) to perform contrastive learning in the embedding space after projection. ℓ_2-normalization is involved for unit-sphere constraint on $\mathbf{z}_i^{\{w;t\}}$.

A reconstructor recovers $\tilde{\mathbf{v}}_i^{\{w;t\}}$ from $\mathbf{z}_i^{\{w;t\}}$, where $\tilde{\mathbf{v}}_i^{\{w;t\}}$ should be as close as possible to $\mathbf{v}_i^{\{w;t\}}$. Symmetric structure is adopted for the projector and reconstructor.

An auxiliary classifier with one FC layer generates probabilities $\mathbf{q}_i^t$ over C classes based on embeddings $\mathbf{z}_i^t$.

Our relation module compares each pair of one instance embedding $\mathbf{z}_i^{\{w;t\}}$ and one class prototype $\mathbf{c}_k \in \mathbb{R}^{d_p}, k \in \{1,...,C\}$ for distance measurement. Given the concatenated embeddings $[\mathbf{z}_i^{\{w;t\}}, \mathbf{c}_k]$, it learns to score their closeness $r_{ik} \in \mathbb{R}$ by two FC layers with one ReLU layer.

Training Strategy

FoPro employs a four-stage training strategy.

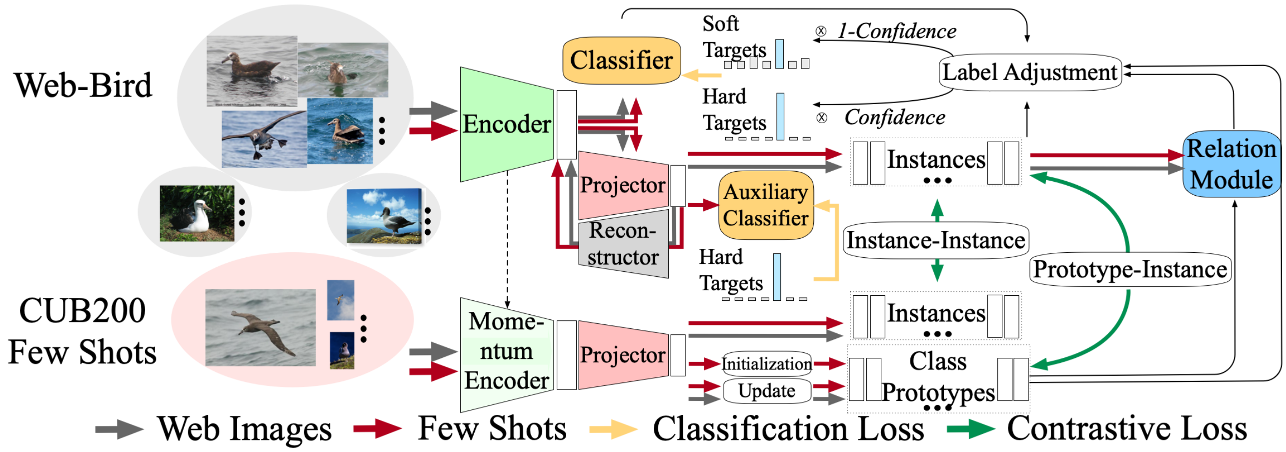

Figure 3: Overview of FoPro. The encoder, classifier, and projector are trained to produce discriminative embeddings. Class prototypes are first initialized by few shots and then polished with clean samples for contrastive learning to regularize cluster distribution. Instance-wise contrastive loss is optimized simultaneously. The relation module learns a distance metric between an instance and its assigned class prototype. Finally, we adjust web labels for confidence-weighted hybrid target learning.

Stage 1: Preparation In this early stage, we warm up the system by learning common, regular patterns for the first T_1 epochs. As discovered by (Arpit et al. 2017), easy examples are reliably learned with simple patterns before the model overfits noise. We achieve this via training the encoder and classifier with cross-entropy loss.

$$\mathcal{L}_i^{cls} = -\log(\mathbf{p}_{i(y_i)}^{\{w;t\}}). \tag{2}$$

Since $\mathbf{v}_i^{\{w;t\}}$ might contain redundant features that make outliers indistinguishable, we set a projector to only keep principal components. The previous method PCL stems from the analogy of autoencoder to PCA, and learns projection by minimizing the reconstruction loss for the projector and reconstructor. In preliminary experiments, however, we find that such optimization cannot give a good starting point for prototype initialization because $\mathbf{z}_i^{\{w;t\}}$ is not necessarily class-indicative. Therefore, an auxiliary classifier is applied on $\mathbf{z}_i^t$ to bring back its representation capacity. Only few shots are used here due to purity concerns.

$$\mathcal{L}_i^{prj} = \|\tilde{\mathbf{v}}_i^{\{w;t\}} - \mathbf{v}_i^{\{w;t\}}\|_2^2 - \log(\mathbf{q}_{i(y_i)}^t). \tag{3}$$

Stage 2: Incubation Clean few shots play an anchoring role in "territory" enclosure in the embedding space. Given extracted embeddings from the momentum encoder, we initialize prototypes by averaging few shots in each class.

$$\hat{\mathbf{c}}_k = \frac{1}{K}\sum_{y_i=k}\mathbf{z}_i^t, \mathbf{c}_k = \frac{\hat{\mathbf{c}}_k}{\|\hat{\mathbf{c}}_k\|_2}. \tag{4}$$

In this stage, we begin to pull instances within one class towards the prototype for T_2 epochs. Besides, instance-level discrimination is encouraged by contrastive losses (Chen et al. 2020a) to improve separation across classes.

$$\mathcal{L}_i^{pro} = -\log\frac{\exp((\mathbf{z}_i^{w;t}\cdot\mathbf{c}_{y_i} - \delta^{w;t})/\phi_{y_i})}{\sum_{k=1}^C \exp((\mathbf{z}_i^{w;t}\cdot\mathbf{c}_k - \delta^{w;t})/\phi_k)}, \tag{5}$$

$$\mathcal{L}_i^{ins} = -\log\frac{\exp(\mathbf{z}_i^{w;t}\cdot\mathbf{z}_i^{\prime w;t}/\tau)}{\sum_{j=1}^Q \exp(\mathbf{z}_i^{w;t}\cdot\mathbf{z}_j^{\prime w;t}/\tau)}, \tag{6}$$

where $\delta^{w;t}$ refers to the margin coefficient, and Q is the length of the memory bank for storing embeddings of visited instances. Temperature coefficients can be fixed as τ or class-dependent as ϕ_k. We put constraints on learning representations with a high margin so that clean few shots gather around prototypes tightly, ensuring better justification and interpretability. Furthermore, to regularize the distribution of each class cluster, adjustable temperature coefficients (Li et al. 2020) are estimated based on concentration.

$$\phi_k = \frac{\sum_{y_i=k}\|\mathbf{z}_i^{w;t} - \mathbf{c}_k\|_2}{N_k^{w;t}\log(N_k^{w;t}+\alpha)}, \tag{7}$$

where $N_k^{w;t}$ denotes the number of web and few-shot instances of class k, and α is a smoother. Embeddings of large, loose clusters will be penalized more to approach their prototypes, while those of small, tight clusters will be relaxed.

Stage 3: Illumination With parameters of the encoder and projector fixed, the relation module learns to score the compatibility between one instance and each prototype. It sheds light on whether the given label of a web image is correct. We select clean samples D^r for training the relation module.

$$D^r = D^t \cup \{(\mathbf{x}_i^w, y_i^w) | \sum_{j=1}^C |(\mathbf{z}_i^w - \mathbf{c}_{y_i})\cdot\mathbf{c}_j| \leq \sigma\}, \tag{8}$$

where σ is a threshold between 0 and 1. Such criterion comprehensively considers both the cosine distance between instance and prototypes, and the distance among prototypes. Then, the relation module is trained for T_3 epochs by:

$$\mathcal{L}_i^{rel} = -\log\frac{\exp(r_{iy_i})}{\sum_{k=1}^C \exp(r_{ik})}. \tag{9}$$

Stage 4: Verification Armed with "pretrained" model, we start label correction, OOD removal, prototype update, and continue noise-robust learning for T_4 epochs. Three sources of prior knowledge are incorporated for cleaning: 1) self-prediction; 2) instance-prototype similarity; 3) relation score. Rules for adjusting labels are detailed below:

$$\mathbf{s}_i^w = \beta \mathbf{p}_i^w + (1-\beta)[\mathbf{c}_1, ..., \mathbf{c}_C]^T \cdot \mathbf{z}_i^w \quad (10)$$

$$\hat{y}_i^w = \begin{cases} y_i^w & \text{if } r_{iy_i} > \gamma, \\ \arg\max_k \mathbf{s}_{i(k)}^w & \text{else if} \max_k \mathbf{s}_{i(k)}^w > \gamma, \\ y_i^w & \text{else if } \mathbf{s}_{i(y_i)}^w > 1/C, \\ \text{Null } (OOD) & \text{otherwise,} \end{cases} \quad (11)$$

where γ is a threshold between 0 and 1. Since fine-grained categories share highly similar visual patterns, the relation module is only used for positive verification of the initial web label. Besides, we introduce an alternative confidence measure from self-prediction and similarity for label reassignment. When the first two conditions are not satisfied, an image will be kept as hard example if its confidence is above average. Otherwise, it is discarded as OOD. Note that the basic control flow above is inspired by MoPro. We further improve it with the proposed relation module (Eq.11 cond. 1) to better evaluate the compatibility between instances and class prototypes, and thereafter enable accurate label-flipping-error correction and OOD removal without ignoring hard examples by mistake (Eq.11 conds. 2–4).

After label adjustment, we exploit the predicted probabilities as pseudo-labels for self-training (Tanaka et al. 2018; Han, Luo, and Wang 2019). Such soft targets can be viewed as a regularizer on the classifier like label smoothing (Müller, Kornblith, and Hinton 2019) and self-knowledge distillation (Hinton et al. 2015). Instead of using a fixed coefficient, we follow (Yang et al. 2020) to leverage confidence on the corrected label for weighting soft and hard targets.

$$\begin{aligned} \mathcal{L}_i^{cls} = \quad & -\log(\mathbf{p}_{i(y_i)}^t) - \mathbf{s}_{i(\hat{y}_i)}^w \log(\mathbf{p}_{i(\hat{y}_i)}^w) \\ & -(1-\mathbf{s}_{i(\hat{y}_i)}^w) \textstyle\sum_{k=1}^C \mathbf{p}_{i(k)}^w \log \mathbf{p}_{i(k)}^w. \end{aligned} \quad (12)$$

With the label-flipping errors and OOD reduced, class prototypes are updated by embeddings of the remaining clean examples from the momentum encoder. Exponential moving average (Li, Xiong, and Hoi 2020) is used for two reasons: 1) initialization by few shots remains to exert a profound anchoring effect. 2) smoothed transition is achieved to stabilize contrastive learning. For class k, web images with $\hat{y}_i^w = k$ and few shot images with $y_i^t = k$ are involved:

$$\hat{\mathbf{c}}_k = m_p \mathbf{c}_k + (1-m_p)\mathbf{z}_i^{w;t}, \mathbf{c}_k = \frac{\hat{\mathbf{c}}_k}{\|\hat{\mathbf{c}}_k\|_2}. \quad (13)$$

Note that reliable samples, which are selected by Eq. 11 per batch, also participate in training the relation module. The criterion by Eq. 8 is only used in stage 3.

Experiments

We train FoPro on web datasets and evaluate it on real-world testing sets. FoPro boosts K-shot performance and reaches the SOTA. Ablation study validates the relation module.

Web Dataset		# Img.	# Cls.	Real-World
Web-FG496	Bird	18k	200	CUB200-2011
	Air	13k	100	FGVC-Aircraft
	Car	21k	196	Stanford Car
Web-Vision1k	Web-Vision1k	2.44M	1k	ImageNet1k
	Google500	0.61M	500	ImageNet500

Table 1: Statistics of web datasets.

Datasets

WebFG496 (Sun et al. 2021) contains three fine-grained datasets sourced from Bing. The testing sets of CUB200-2011 (Wah et al. 2011), FGVC-Aircraft (Maji et al. 2013), and Stanford Car (Krause et al. 2013) are used.

WebVision1k (Li et al. 2017) is collected from Google and Flickr. The validation set of ImageNet1k (Deng et al. 2009) is used. Besides, we also use **Google500** (Yang et al. 2020) where 500 out of 1k categories are randomly sampled with images only from Google (see Table 1).

We randomly sample K shots per class from the training sets of real-world datasets. Classification accuracy (%) is adopted as the evaluation metric for all experiments.

Implementation Details

WebFG496 The B-CNN (Lin, RoyChowdhury, and Maji 2015) (VGG-16 (Simonyan and Zisserman 2014)) is used as encoder. We refer to (Sun et al. 2021) for the training settings: optimizer is Adam with weight decay of 1×10^{-8}; batch size is 64; the learning rate is 1×10^{-4} and decays to 0 by cosine schedule; a warm-up policy increases the learning rate linearly for 5 epochs with the frozen encoders.

WebVision1k The ResNet-50 (R50) (He et al. 2016) is used as encoder. We refer to (Yang et al. 2020) for the training settings: batch size is 256; optimizer is SGD with the momentum of 0.9 and weight decay of 1×10^{-4}; the learning rate is 0.01 and decays to 0 by cosine schedule.

We refer to MoPro to set $m_e = 0.999$, $m_p = 0.999$, $d_p = 128$, and $Q = 8192$. In view of the dataset scale, we set $T_1 = 20$, $T_2 = 5$, $T_3 = 20$, $T_4 = 175$ for WebFG496 and set $T_1 = 15$, $T_2 = 5$, $T_3 = 10$, $T_4 = 30$ for WebVision1k/Google500. Preliminary experiments on WebFG496 show that $\gamma = 0.6$ and $\beta = 0.5$ work better than $\gamma = 0.2$ and $\beta = 0, 0.25, 0.75, 1$. A lower γ means a more relaxed criterion on clean sample selection, which might bring in noise and cause performance drop. The balanced combination of self-prediction and similarity terms performs more robust to noise than the biased cases. Other hyper-parameters are empirically set as: $\delta^w = 0$, $\delta^t = 0.5$, $\tau = 0.1$, $\alpha = 10$, $\sigma = 20$. Their optimal values require meticulous fine-tuning, which is beyond consideration of the present study.

Data augmentation includes random cropping and horizontal flipping. Strong augmentation on the inputs to the momentum encoder (He et al. 2020) additionally uses color jittering and blurring. Since birds might only differ in color, random rotation in 45 degrees is used instead. Experiments are conducted on a CentOS 7 workstation with an Intel 8255C CPU, 377 GB Mem, and 8 NVIDIA V100 GPUs.

Results

Method	Back-bone	WebFG496 Bird	Air	Car	Avg.
Vanilla	R50	64.43	60.79	60.64	61.95
MoPro†	R50	71.16	76.85	79.68	75.90
SCC†	R50-D	61.10	74.92	83.49	73.17
Vanilla	B-CNN	66.56	64.33	67.42	66.10
Decouple	B-CNN	70.56	75.97	75.00	73.84
CoTeach	B-CNN	73.85	72.76	73.10	73.24
PeerLearn	B-CNN	76.48	74.38	78.52	76.46
PeerLearn†	B-CNN	76.57	74.35	78.26	76.39
FoPro(K=0)	B-CNN	77.79	79.37	86.99	81.38
FoPro(K=1)	B-CNN	78.07	79.87	88.01	82.03
FoPro(K=16)	B-CNN	**85.54**	**86.40**	**91.51**	**87.81**

† Results are reproduced by ourselves with the official codes.

Table 2: The SOTA results on fine-grained datasets.

Baselines Our FoPro is compared with vanilla backbones and the SOTA methods including SCC, MoPro, Decouple (Malach and Shalev-Shwartz 2017), CoTeach (Han et al. 2018), PeerLearn, MentorNet (Jiang et al. 2018), CurriculumNet (Guo et al. 2018), and CleanNet (Lee et al. 2018). Results of the SOTA methods that are trained and evaluated on the same datasets are directly quoted here. We also reproduce three closely-related methods of SCC, MoPro, and PeerLearn under K-shot settings with the officially released codes. Their default hyper-parameters are employed if the same web datasets are engaged. Otherwise, they are set the same as ours. Additionally, we modify the proposed method only to exhibit its applicability for 0-shot without specific design. In that case, web images with predicted probability of the target class over γ are used to train the auxiliary classifier. In view of the dataset scale, prototypes are initialized by randomly sampled 16 and 50 web images per class from WebFG496 and WebVision1k/Google500, respectively.

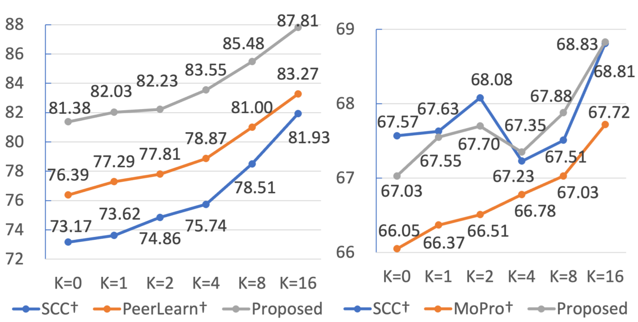

Figure 4: The averaged results under K-shot settings on fine-grained datasets (left) and ImageNet1k (right).

Table 2 confirms the superiority of the proposed method on fine-grained datasets even under 0-shot. FoPro boosts the accuracy of vanilla backbones more significantly than the SOTA methods with respect to their backbones.

Method†	Back-bone	ImageNet1k Top 1	ImageNet1k Top 5	ImageNet500 Top 1	ImageNet500 Top 5
MentorNet	Inception ResNetV2	64.20	84.80	–	–
Curriculum-Net	Inception V2	64.80	83.40	–	–
Vanilla	R50-D	67.23	84.09	–	–
SCC	R50-D	67.93	84.77	68.84	84.62
SCC†	R50-D	67.57	85.74	64.40	81.56
Vanilla	R50	65.70	85.10	61.54	78.89
CoTeach	R50	–	–	62.18	80.98
CleanNet	R50	63.42	84.59	–	–
MoPro	R50	67.80	87.00	–	–
MoPro†	R50	66.05	85.66	58.68	78.39
PeerLearn†	R50	52.57	73.35	42.04	61.71
FoPro(K=0)	R50	67.03	85.57	68.59	86.03
FoPro(K=1)	R50	67.55	86.31	69.11	86.19
FoPro(K=16)	R50	**68.83**	**87.83**	**72.02**	**89.38**

† Results are reproduced by ourselves with the official codes.

Table 3: The SOTA results on large-scale datasets.

FoPro reaches the optimal performance on large-scale datasets with K=16 (see Table 3). The vanilla R50-D (He et al. 2019) performs better than R50. Although FoPro is preceded by SCC and MoPro at first (0-shot), it rises steadily after exploiting a few real-world examples efficiently.

Under the degeneration circumstance (K=0), FoPro outperforms the SOTA methods on WebFG496. The reason why FoPro (K=0) degrades slightly on ImageNet1k/500 lies in the high percentage of noises in WebVision1k/Google500. In that case, prototypes (K=0) are initialized and polished solely by noisy web examples without intervention from clean shots, which may not be class-representative. With few real-world examples ($K > 0$) involved, FoPro regains its advantage over the SOTA methods.

K	WebFG496 Avg. Top 1	Gap	ImageNet1k Top 1	Gap	ImageNet500 Top 1	Gap
0	81.38	–	67.03	5.57	68.59	3.85
1	+0.65	–	+0.52	5.22	+0.52	3.63
2	+0.85	–	+0.67	5.20	+1.35	3.29
4	+2.17	–	+0.32	4.60	+1.50	2.91
8	+4.10	–	+0.85	4.64	+2.06	2.90
16	+6.43	–	+1.80	3.91	+3.43	2.19
16	87.81	–	68.83	–	72.02	–
Ref.	87.16†	–	76.15‡	–	76.22‡	–

† Official results of the B-CNN trained on FGVC-Aircraft, CUB200-2011, and Stanford Car are averaged.

‡ Official results of the R50 trained on ImageNet1k by PyTorch are quoted respectively for 500 and 1k classes.

Table 4: FoPro gains of K-shot over 0-shot. Gap refers to the differences between web and real-world testing results.

Effect of Few-Shots We explore the potential of FoPro by varying the number of real-world examples per class from 1 to 16. As shown in Fig. 4, FoPro achieves consistent performance growth with K on fine-grained datasets. It surpasses

Figure 5: One-shot real-world examples and the web images sorted by their distance to class prototypes. Best viewed magnified.

SCC and PeerLearn by a large margin. On ImageNet1k, the abnormal case of K=4 is mainly due to sampling jittering. Since ImageNet contains many unreal images, it could not eliminate the possibility of sampling atypical images of certain classes. However, as K increases, FoPro starts to take the lead. We believe more few shots directly refine the estimated prototypes for better representation. Clean samples can be more appropriately selected to promote discriminative feature learning. With amendment on cluster formation, FoPro also enjoys a higher level of interpretability in class centers with competitive performance.

Table 4 reports the performance gap between WebVision1k/ImageNet1k and Google500/ImageNet500 when the testing sets of web domain are available. In line with Fig. 2(b), the reduced gap reflects that we bridge the noisy web domain and real-world domain with limited K shots. FoPro approaches reference benchmarks that are trained on real-world datasets, corroborating its practical value that much labor of data collection and annotation can be saved.

Effect of Relation Module In Table 5, we study the effect of relation module for clean example selection. We remove FC layers and directly compare an instance and each prototype using cosine similarity. Results confirm that the proposed relation module discovers clean examples more precisely than the pre-defined similarity metric. By using a non-linear metric, we do not assume that element-wise comparison could solely separate matching or mismatching pairs. Besides, such a learnable metric is not sensitive to input variation and behaves better on noisy samples.

K=1	WebFG496 Avg.	ImageNet1k	ImageNet500
w/o RM	81.59	65.22	64.69
w RM	82.03	67.55	69.11

Table 5: Ablation Study on the Relation Module (RM).

Visualization In Fig. 2(a), we visualize the low-dimensional embeddings with t-SNE for the randomly chosen 10 categories in WebVision as a demonstration. For convenience, all 16 real-world examples in each class are averaged and displayed as one few-shot example. Differences in the cluster distribution (from K=1 to K=16) are highlighted to show that: 1) the distance between each prototype and the few-shot example becomes shorter; 2) the density of class clusters is improved. From Fig. 5, we conclude the following insights: 1) Web images close to the estimated prototypes are clean and similar to real-world photos with limited post-processing. Our FoPro learns to sort out noise in web data for robust representation learning. 2) The proposed method generalizes across various domains such as product close-up, computer graphics, and screenshots. 3) Intra-class diversity (*e.g.*, wing postures of the sooty albatross), uncaptured salient parts (*e.g.*, the yellowish patch on the back head of the bobolink), and editing of tone curve (*e.g.*, colored body of the painted bunting and yellow-breasted chat) are the possible reasons why hard examples of 1-shot and clean web images still locate away from prototypes.

Conclusion

This paper introduces a new setting for webly-supervised learning, which optimizes the learning system with a large quantity of noisy web images and a few real-world images. Under this setting, we propose a few-shot guided prototypical representation learning method called FoPro, which simultaneously tackles noise and dataset bias in a cost-efficient manner. It is characterized by the guidance from a few real-world domain images for learning noise-robust and generalizable representations from web data. Experimental results demonstrate that our method can effectively utilize few-shot images to improve the performance of WSL on real-world benchmarks. Future work includes investigation of side information from web datasets (*e.g.*, captions, website titles, and user comments) and application extension to weakly-supervised object detection and segmentation.

References

Arpit, D.; Jastrzebski, S.; Ballas, N.; Krueger, D.; Bengio, E.; Kanwal, M. S.; Maharaj, T.; Fischer, A.; Courville, A.; Bengio, Y.; et al. 2017. A closer look at memorization in deep networks. In *International Conference on Machine Learning*, 233–242. PMLR.

Bergamo, A.; and Torresani, L. 2010. Exploiting weakly-labeled web images to improve object classification: a domain adaptation approach. *Advances in Neural Information Processing Systems*, 23.

Chen, T.; Kornblith, S.; Norouzi, M.; and Hinton, G. 2020a. A simple framework for contrastive learning of visual representations. In *International Conference on Machine Learning*, 1597–1607. PMLR.

Chen, X.; Fan, H.; Girshick, R.; and He, K. 2020b. Improved baselines with momentum contrastive learning. *arXiv preprint arXiv:2003.04297*.

Chen, X.; and Gupta, A. 2015. Webly supervised learning of convolutional networks. In *Proceedings of the IEEE international conference on computer vision*, 1431–1439.

Cheng, L.; Zhou, X.; Zhao, L.; Li, D.; Shang, H.; Zheng, Y.; Pan, P.; and Xu, Y. 2020. Weakly supervised learning with side information for noisy labeled images. In *European Conference on Computer Vision*, 306–321. Springer.

Deng, J.; Dong, W.; Socher, R.; Li, L.-J.; Li, K.; and Fei-Fei, L. 2009. ImageNet: A large-scale hierarchical image database. In *Proceedings of the IEEE/CVF International Conference on Computer Vision*, 248–255. IEEE.

Divvala, S. K.; Farhadi, A.; and Guestrin, C. 2014. Learning everything about anything: Webly-supervised visual concept learning. In *Proceedings of the IEEE Conference on Computer Vision and Pattern Recognition*, 3270–3277.

Ghosh, A.; Kumar, H.; and Sastry, P. S. 2017. Robust loss functions under label noise for deep neural networks. In *Proceedings of the AAAI Conference on Artificial Intelligence*, volume 31.

Guo, S.; Huang, W.; Zhang, H.; Zhuang, C.; Dong, D.; Scott, M. R.; and Huang, D. 2018. CurriculumNet: Weakly supervised learning from large-scale web images. In *European Conference on Computer Vision*, 135–150.

Han, B.; Yao, Q.; Yu, X.; Niu, G.; Xu, M.; Hu, W.; Tsang, I.; and Sugiyama, M. 2018. Co-teaching: Robust Training of Deep Neural Networks with Extremely Noisy Labels. *Advances in Neural Information Processing Systems*, 31.

Han, J.; Luo, P.; and Wang, X. 2019. Deep self-learning from noisy labels. In *Proceedings of the IEEE/CVF Conference on Computer Vision and Pattern Recognition*, 5138–5147.

He, K.; Fan, H.; Wu, Y.; Xie, S.; and Girshick, R. 2020. Momentum contrast for unsupervised visual representation learning. In *Proceedings of the IEEE/CVF Conference on Computer Vision and Pattern Recognition*, 9729–9738.

He, K.; Zhang, X.; Ren, S.; and Sun, J. 2016. Deep residual learning for image recognition. In *Proceedings of the IEEE/CVF International Conference on Computer Vision*, 770–778.

He, T.; Zhang, Z.; Zhang, H.; Zhang, Z.; Xie, J.; and Li, M. 2019. Bag of tricks for image classification with convolutional neural networks. In *Proceedings of the IEEE/CVF Conference on Computer Vision and Pattern Recognition*, 558–567.

Hinton, G.; Vinyals, O.; Dean, J.; et al. 2015. Distilling the knowledge in a neural network. *arXiv preprint arXiv:1503.02531*, 2(7).

Jiang, L.; Zhou, Z.; Leung, T.; Li, L.-J.; and Fei-Fei, L. 2018. MentorNet: Learning data-driven curriculum for very deep neural networks on corrupted labels. In *International Conference on Machine Learning*, 2304–2313. PMLR.

Jin, B.; Ortiz Segovia, M. V.; and Susstrunk, S. 2017. Webly supervised semantic segmentation. In *Proceedings of the IEEE/CVF Conference on Computer Vision and Pattern Recognition*, 3626–3635.

Kaur, P.; Sikka, K.; and Divakaran, A. 2017. Combining weakly and webly supervised learning for classifying food images. *arXiv preprint arXiv:1712.08730*.

Kim, D.; Cho, D.; Yoo, D.; and Kweon, I. S. 2018. Learning image representations by completing damaged jigsaw puzzles. In *IEEE Winter Conference on Applications of Computer Vision*, 793–802. IEEE.

Kolesnikov, A.; Beyer, L.; Zhai, X.; Puigcerver, J.; Yung, J.; Gelly, S.; and Houlsby, N. 2019. Large scale learning of general visual representations for transfer. *arXiv preprint arXiv:1912.11370*, 2(8).

Krause, J.; Sapp, B.; Howard, A.; Zhou, H.; Toshev, A.; Duerig, T.; Philbin, J.; and Fei-Fei, L. 2016. The unreasonable effectiveness of noisy data for fine-grained recognition. In *European Conference on Computer Vision*, 301–320. Springer.

Krause, J.; Stark, M.; Deng, J.; and Fei-Fei, L. 2013. 3d object representations for fine-grained categorization. In *Proceedings of the IEEE/CVF International Conference on Computer Vision Workshops*, 554–561.

Lee, K.-H.; He, X.; Zhang, L.; and Yang, L. 2018. CleanNet: Transfer Learning for Scalable Image Classifier Training with Label Noise. In *Proceedings of the IEEE/CVF Conference on Computer Vision and Pattern Recognition*, 5447–5456.

Li, J.; Socher, R.; and Hoi, S. C. 2019. DivideMix: Learning with Noisy Labels as Semi-supervised Learning. In *International Conference on Learning Representations*.

Li, J.; Xiong, C.; and Hoi, S. 2020. MoPro: Webly Supervised Learning with Momentum Prototypes. In *International Conference on Learning Representations*.

Li, J.; Zhou, P.; Xiong, C.; and Hoi, S. 2020. Prototypical Contrastive Learning of Unsupervised Representations. In *International Conference on Learning Representations*.

Li, W.; Wang, L.; Li, W.; Agustsson, E.; and Van Gool, L. 2017. WebVision database: Visual learning and understanding from web data. *arXiv preprint arXiv:1708.02862*.

Lin, T.-Y.; RoyChowdhury, A.; and Maji, S. 2015. Bilinear CNN models for fine-grained visual recognition. In *Proceedings of the IEEE/CVF International Conference on Computer Vision*, 1449–1457.

Liu, H.; Zhang, H.; Lu, J.; and Tang, Z. 2021. Exploiting Web Images for Fine-Grained Visual Recognition via Dynamic Loss Correction and Global Sample Selection. *IEEE Transactions on Multimedia*, 24: 1105–1115.

Maji, S.; Rahtu, E.; Kannala, J.; Blaschko, M.; and Vedaldi, A. 2013. Fine-grained visual classification of aircraft. *arXiv preprint arXiv:1306.5151*.

Malach, E.; and Shalev-Shwartz, S. 2017. Decoupling" when to update" from" how to update". *Advances in Neural Information Processing Systems*, 30.

Müller, R.; Kornblith, S.; and Hinton, G. E. 2019. When does label smoothing help? *Advances in Neural Information Processing Systems*, 32.

Niu, L.; Li, W.; and Xu, D. 2015. Visual recognition by learning from web data: A weakly supervised domain generalization approach. In *Proceedings of the IEEE Conference on Computer Vision and Pattern Recognition*, 2774–2783.

Pereyra, G.; Tucker, G.; Chorowski, J.; Kaiser, Ł.; and Hinton, G. 2017. Regularizing neural networks by penalizing confident output distributions. *arXiv preprint arXiv:1701.06548*.

Reed, S. E.; Lee, H.; Anguelov, D.; Szegedy, C.; Erhan, D.; and Rabinovich, A. 2015. Training Deep Neural Networks on Noisy Labels with Bootstrapping. In *International Conference on Learning Representations (Workshop)*.

Shen, T.; Lin, G.; Shen, C.; and Reid, I. 2018. Bootstrapping the performance of webly supervised semantic segmentation. In *Proceedings of the IEEE/CVF Conference on Computer Vision and Pattern Recognition*, 1363–1371.

Shen, Y.; Ji, R.; Chen, Z.; Hong, X.; Zheng, F.; Liu, J.; Xu, M.; and Tian, Q. 2020. Noise-aware fully webly supervised object detection. In *Proceedings of the IEEE/CVF Conference on Computer Vision and Pattern Recognition*, 11326–11335.

Simonyan, K.; and Zisserman, A. 2014. Very deep convolutional networks for large-scale image recognition. *arXiv preprint arXiv:1409.1556*.

Song, H.; Kim, M.; Park, D.; Shin, Y.; and Lee, J.-G. 2022. Learning from noisy labels with deep neural networks: A survey. *IEEE Transactions on Neural Networks and Learning Systems*.

Sun, C.; Shrivastava, A.; Singh, S.; and Gupta, A. 2017. Revisiting unreasonable effectiveness of data in deep learning era. In *Proceedings of the IEEE/CVF International Conference on Computer Vision*, 843–852.

Sun, Z.; Yao, Y.; Wei, X.-S.; Zhang, Y.; Shen, F.; Wu, J.; Zhang, J.; and Shen, H. T. 2021. Webly supervised fine-grained recognition: Benchmark datasets and an approach. In *Proceedings of the IEEE/CVF International Conference on Computer Vision*, 10602–10611.

Tanaka, D.; Ikami, D.; Yamasaki, T.; and Aizawa, K. 2018. Joint optimization framework for learning with noisy labels. In *Proceedings of the IEEE/CVF Conference on Computer Vision and Pattern Recognition*, 5552–5560.

Tu, Y.; Niu, L.; Chen, J.; Cheng, D.; and Zhang, L. 2020. Learning from web data with self-organizing memory module. In *Proceedings of the IEEE/CVF Conference on Computer Vision and Pattern Recognition*, 12846–12855.

Van der Maaten, L.; and Hinton, G. 2008. Visualizing data using t-SNE. *Journal of Machine Learning Research*, 9(11).

Wah, C.; Branson, S.; Welinder, P.; Perona, P.; and Belongie, S. 2011. The caltech-ucsd birds-200-2011 dataset. Technical Report CNS-TR-2011-001, California Institute of Technology.

Wang, R.; Liu, T.; and Tao, D. 2017. Multiclass learning with partially corrupted labels. *IEEE Transactions on Neural Networks and Learning Systems*, 29(6): 2568–2580.

Wu, Z.-F.; Wei, T.; Jiang, J.; Mao, C.; Tang, M.; and Li, Y.-F. 2021. NGC: a unified framework for learning with open-world noisy data. In *Proceedings of the IEEE/CVF International Conference on Computer Vision*, 62–71.

Xiao, T.; Xia, T.; Yang, Y.; Huang, C.; and Wang, X. 2015. Learning from massive noisy labeled data for image classification. In *Proceedings of the IEEE/CVF Conference on Computer Vision and Pattern Recognition*, 2691–2699.

Xu, Z.; Huang, S.; Zhang, Y.; and Tao, D. 2016. Webly-supervised fine-grained visual categorization via deep domain adaptation. *IEEE Transactions on Pattern Analysis and Machine Intelligence*, 40(5): 1100–1113.

Yang, J.; Feng, L.; Chen, W.; Yan, X.; Zheng, H.; Luo, P.; and Zhang, W. 2020. Webly supervised image classification with self-contained confidence. In *European Conference on Computer Vision*, 779–795. Springer.

Yao, Y.; Hua, X.; Gao, G.; Sun, Z.; Li, Z.; and Zhang, J. 2020. Bridging the web data and fine-grained visual recognition via alleviating label noise and domain mismatch. In *Proceedings of the ACM International Conference on Multimedia*, 1735–1744.

Yao, Y.; Zhang, J.; Shen, F.; Hua, X.; Xu, J.; and Tang, Z. 2017. Exploiting web images for dataset construction: A domain robust approach. *IEEE Transactions on Multimedia*, 19(8): 1771–1784.

Zhang, C.; Bengio, S.; Hardt, M.; Recht, B.; and Vinyals, O. 2021. Understanding deep learning (still) requires rethinking generalization. *Communications of the ACM*, 64(3): 107–115.

Zhang, C.; Yao, Y.; Liu, H.; Xie, G.-S.; Shu, X.; Zhou, T.; Zhang, Z.; Shen, F.; and Tang, Z. 2020. Web-supervised network with softly update-drop training for fine-grained visual classification. In *Proceedings of the AAAI Conference on Artificial Intelligence*, volume 34, 12781–12788.

Zhang, H.; Cisse, M.; Dauphin, Y. N.; and Lopez-Paz, D. 2018. MixUp: Beyond Empirical Risk Minimization. In *International Conference on Learning Representations*.

Zhang, Z.; and Sabuncu, M. 2018. Generalized Cross Entropy Loss for Training Deep Neural Networks with Noisy Labels. *Advances in Neural Information Processing Systems*, 31.

Zhou, X.; Pan, P.; Zheng, Y.; Xu, Y.; and Jin, R. 2020. Large scale long-tailed product recognition system at alibaba. In *Proceedings of ACM International Conference on Information & Knowledge Management*, 3353–3356.